

# Spatially unassociated galaxies contribute significantly to the blended submillimetre galaxy population: predictions for follow-up observations of ALMA sources

Christopher C. Hayward<sup>1\*</sup>, Peter S. Behroozi<sup>2,3</sup>, Rachel S. Somerville<sup>4</sup>, Joel R. Primack<sup>5</sup>, Jorge Moreno<sup>6†</sup>, and Risa H. Wechsler<sup>2,3</sup>

<sup>1</sup>Heidelberg Institut für Theoretische Studien, Schloss–Wolfsbrunnenweg 35, 69118 Heidelberg, Germany

<sup>2</sup>Kavli Institute for Particle Astrophysics and Cosmology, Department of Physics, Stanford University, Stanford, CA 94305, USA

<sup>3</sup>Department of Particle Physics and Astrophysics, SLAC National Accelerator Laboratory, Menlo Park, CA 94025, USA

<sup>4</sup>Department of Physics & Astronomy, Rutgers University, 136 Frelinghuysen Road, Piscataway, NJ 08854, USA

<sup>5</sup>Department of Physics, University of California at Santa Cruz, Santa Cruz, CA 95064, USA

<sup>6</sup>Department of Physics & Astronomy, University of Victoria, 3800 Finnerty Road, Victoria, BC V8P 5C2, Canada

Accepted for publication in MNRAS

## ABSTRACT

There is anecdotal evidence that spatially and physically unassociated galaxies blended into a single submillimetre (submm) source contribute to the submm galaxy (SMG) population. This work is the first to theoretically predict the number counts of such sources. We generate mock SMG catalogues using lightcones derived from the *Bolshoi* cosmological simulation; to assign submm flux densities to the mock galaxies, we use a fitting function previously derived from the results of dust radiative transfer performed on hydrodynamical simulations of isolated disc and merging galaxies. We then calculate submm number counts for different beam sizes and without blending. We predict that  $\gtrsim 50$  per cent of blended SMGs have at least one spatially unassociated component with  $S_{850} > 1$  mJy. For a 15-arcsec beam, blends of  $> 2$  galaxies in which at least one component is spatially unassociated dominate the blended sources with total  $S_{850} \gtrsim 3$  mJy. The distribution of the redshift separations amongst the components is strongly bimodal. The typical redshift separation of spatially unassociated blended sources is  $\sim 1$ . Our predictions for the contributions of spatially unassociated components and the distribution of redshift separations are not testable with currently available data, but they will be easily tested once sufficiently accurate redshifts for the individual subcomponents (resolved by, e.g., ALMA) of a sufficient number of single-dish-detected blended SMGs are available.

**Key words:** galaxies: abundances – galaxies: high-redshift – galaxies: luminosity function, mass function – cosmology: theory – cosmology: large-scale structure of Universe – submillimetre: galaxies.

## 1 INTRODUCTION

Submillimetre (submm) galaxies<sup>1</sup> (SMGs; see Blain et al. 2002 for a review) are some of the most luminous, rapidly star-forming galaxies (with star formation rates of  $\sim 10^2 - 10^3 M_{\odot} \text{ yr}^{-1}$ ; e.g., Magnelli et al. 2010, 2012; Chapman et al. 2010; Michałowski et al. 2010a,b) in the Universe. Although simulations have suggested that merger-induced starbursts can pro-

duce the submm fluxes characteristic of SMGs (Chakrabarti et al. 2008; Narayanan et al. 2009, 2010a,b; Hayward et al. 2011a), explaining the observed number density of such prodigious star-formers has posed a challenge for semi-analytic models and hydrodynamical simulations (e.g., Granato et al. 2000; Baugh et al. 2005; Fontanot et al. 2007; Davé et al. 2010; Hayward et al. 2011b, 2013; Narayanan, Bothwell, & Davé 2012; Narayanan & Davé 2012; Niemi et al. 2012; Shimizu, Yoshida, & Okamoto 2012; Somerville et al. 2012), which has caused some to consider them a challenge for  $\Lambda$ CDM (Primack 2012).

Recently, Hayward et al. (2011a, 2012, 2013) suggested that treatment of the effects of blending caused by the large beam sizes (FWHM  $\sim 15$  arcsec, or  $\sim 130$  kpc at  $z \sim 2 - 3$ ) of the single-dish telescopes used to identify SMGs can help alleviate the discrepancy between the SMG number counts predicted by mod-

\* E-mail: christopher.hayward@h-its.org

† CITA National Fellow

<sup>1</sup> Throughout this work, we use the acronym SMG in the conventional manner – to denote single-dish-detected submm sources – although a given SMG may be composed of multiple distinct galaxies. This issue is discussed in Section 4.2.

els and those observed. Specifically, during the pre-coalescence phase of major mergers, both progenitor discs can be blended into a single submm source; Hayward et al. (2013, hereafter, H13) suggest that such ‘galaxy-pair’ SMGs account for a significant fraction ( $\gtrsim 30$  per cent) of the SMG population. Interferometric observations (e.g., Tacconi et al. 2006, 2008; Bothwell et al. 2010; Riechers et al. 2011a,b; Engel et al. 2010; Wang et al. 2011; Barger et al. 2012; Smolčić et al. 2012a; Karim et al. 2013) have provided many examples of single-dish SMGs that are resolved into multiple components when observed at an order-of-magnitude better resolution, and in some cases, the redshifts and kinematics suggest that the individual sources are widely separated (projected separation  $\gtrsim 10$  kpc) discs in the process of merging. Recent interferometric continuum imaging surveys suggest that of order half of single-dish-detected SMGs are blends of two or more distinct components (Smolčić et al. 2012a; Karim et al. 2013). Interestingly, in those surveys, the brightest sources (those with 870- $\mu\text{m}$  flux density  $S_{870} \gtrsim 12$  mJy) are almost all blended sources. However, there are at least fifteen examples of interferometrically observed sources that are brighter than the suggested flux density cutoffs (e.g., Dannerbauer et al. 2002; Younger et al. 2007, 2008a,b, 2009a; Barger et al. 2012; Hodge et al. 2012; Smolčić et al. 2012b; Wagg et al. 2012; see Hayward 2013 for further details). Thus, the fraction of single-dish submm sources that are blended and the brightest submm flux density of a single galaxy are still uncertain.

A submm flux-density cutoff suggests an upper limit on the star formation rate (SFR) of SMGs (Karim et al. 2013; Hayward 2013), which may be a consequence of feedback from star formation and/or active galactic nuclei but may also be simply a consequence of limited gas supply. It also suggests that to reproduce the brightest SMGs, models must account for the effects of blending. In this work, one question that we address is whether we can reproduce the number counts of the brightest SMGs via blended sources alone.

Early-stage mergers are only one type of blended submm source; it is also possible that spatially (and thus physically) unassociated projected multiples contribute to the SMG population. There is already anecdotal evidence for this subpopulation: Wang et al. (2011) present two examples of SMGs that are resolved into multiple components by the Submillimeter Array (SMA) and for which the resolved components are located at significantly different redshifts (in one case, the difference between the two components is  $\Delta z = 1.015$ , and in the other, the three components have redshifts of 2.914, 3.157, and 3.46). Thus, the individual components are not widely separated galaxies that will merge but rather chance projections of completely unrelated galaxies. Some of the sources observed by Smolčić et al. (2012a) may also be examples of this subpopulation.

The relative contribution of such projected multiples to the SMG population is currently unconstrained. However, this situation is likely to change soon, once redshifts for a significant number of the sources from the Atacama Large Millimeter/submillimeter Array (ALMA) follow-up observations (Karim et al. 2013; Hodge et al. 2013) of the Large APEX Bolometer Camera (LABOCA; Siringo et al. 2009) Extended *Chandra* Deep Field South Submillimetre Survey (LESS; Weiß et al. 2009) sources are available. Thus, a prediction for the relative contributions of spatially associated and unassociated components is particularly timely.

In this work, we make such a prediction. To do so, we use halo catalogues derived from a cosmological simulation. Stellar masses and SFRs are assigned using observationally constrained stellar

mass– and SFR–halo mass relations. For each galaxy, we assign an 850- $\mu\text{m}$  flux density  $S_{850}$  using a fitting function, which was previously derived from the results of dust radiative transfer performed on hydrodynamical simulations of isolated disc and merging galaxies, that gives  $S_{850}$  as a function of SFR and dust mass. Then, we search the mock catalogues for blended submm sources and calculate the total submm flux density for each blended source. Using a cut based on the redshift separations of the individual components of the blended sources, we separate the blended sources into ‘spatially associated’ and ‘spatially unassociated’ subpopulations and calculate the relative contributions to the submm number counts as a function of single-dish submm flux density.

The remainder of this work is organised as follows: in Section 2, we discuss the details of our method. In Section 3, we present our predictions for the cumulative submm number counts for different beam sizes, the relative contributions of spatially associated and unassociated sources, and the distribution of redshift separations amongst the individual components of blended sources. In Section 4, we discuss some implications of our results. Section 5 presents our conclusions and plans for future work.

## 2 METHODS

### 2.1 Creating mock galaxy catalogues

The method used in this work differs significantly from that of H13 because the method used in H13 cannot treat spatially unassociated projected multiples. Here, we use mock lightcones derived from a cosmological simulation to provide information about the large-scale clustering of dark matter haloes. We start with halo catalogues from the *Bolshoi* simulation (Klypin, Trujillo-Gomez, & Primack 2011; Behroozi et al. 2013b,c), which is a collisionless dark matter simulation performed using the Adaptive Refinement Tree (ART; Kravtsov, Klypin, & Khokhlov 1997) code. The *Bolshoi* simulation volume has side length  $250 h^{-1}$  Mpc and contains  $2048^3$  particles, which yields a mass resolution of  $1.35 \times 10^8 h^{-1} M_{\odot}$ . The force resolution is  $1 h^{-1}$  kpc (physical). The cosmological parameters used for *Bolshoi* are  $\Omega_m = 0.27$ ,  $\Omega_{\Lambda} = 0.73$ ,  $h = 0.7$ ,  $\sigma_8 = 0.82$ , and  $n_s = 0.95$ . These parameters are consistent with the WMAP7+BAO+ $H_0$  results (Komatsu et al. 2011). The values for  $\sigma_8$  and  $n_s$  are also consistent with the recent *Planck* results (Planck Collaboration et al. 2013a,b). The value of  $\Omega_m$  ( $\Omega_{\Lambda}$  and  $h$ ) used is  $2.6\sigma$  greater ( $2.2\sigma$  less) than that from *Planck*. Nevertheless, the uncertainty in the cosmological parameters should affect our results less than the other uncertainties discussed below.

Starting at eight random locations within the simulation volume, we select haloes along a randomly oriented sightline with an  $84' \times 84'$  ( $1.96 \text{ deg}^2$ ) field of view from  $z = 0.5$  to  $z = 8$ ; this redshift range contains the bulk of the SMG population, both in the real Universe (e.g., Smolčić et al. 2012a; Yun et al. 2012; Michałowski et al. 2012; Weiß et al. 2013) and in our model (for reasons discussed below). Cosmological redshifts are calculated including the effects of halo peculiar velocities. Stellar masses are assigned based on the stellar mass–halo mass relation of Behroozi, Wechsler, & Conroy (2013a), which accounts for redshift-dependent scatter in stellar mass at fixed halo mass and the effects of systematic observational biases in stellar mass recovery. SFRs are assigned based on the SFR–halo mass relation of Behroozi et al. (2013a); this includes redshift-dependent scatter in SFRs at fixed halo mass and the increasingly tight correlation between stellar mass and SFR at fixed halo mass at high redshifts. To

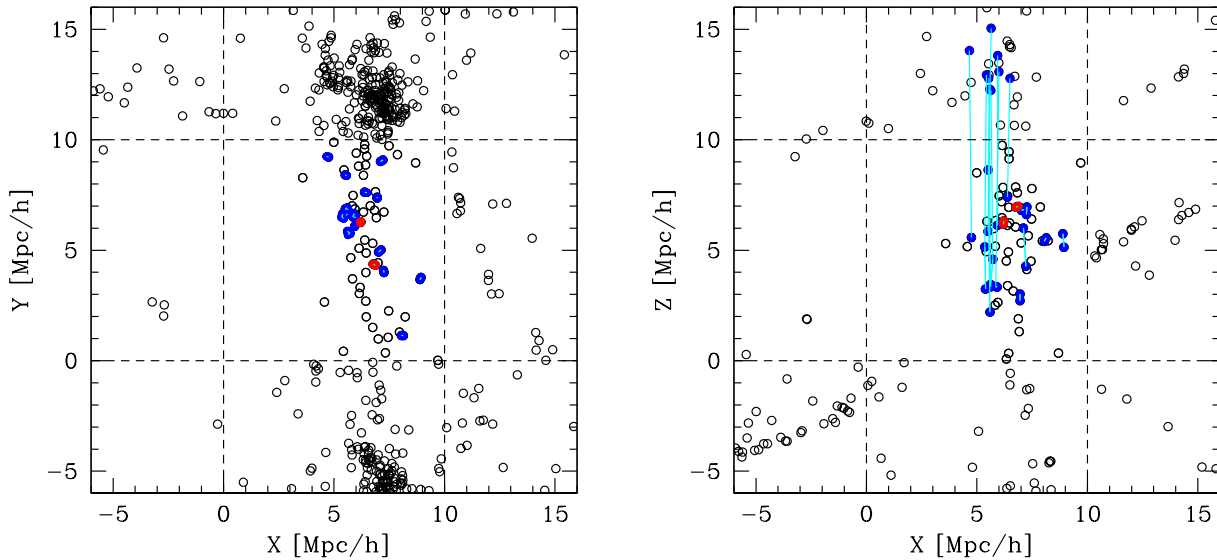


**Figure 1.** Demonstration of the difference between spatially associated and spatially unassociated galaxy pairs. Open circles denote the locations of mock galaxies, and dashed lines demarcate cubic regions with side length  $10 h^{-1}$  Mpc (comoving). The focus is on galaxies in the central cube and their neighbours (which may be located in the neighbouring cubic regions). *Left:*  $X$ - $Y$  plane. Red solid symbols denote galaxies that are associated in three dimensions, whereas blue solid symbols denote galaxies that appear to be associated in projection but are actually unassociated in three dimensions. An observer without access to accurate redshifts would be unable to distinguish between these two cases. *Right:*  $X$ - $Z$  plane. This rotated perspective verifies that the galaxy pairs denoted with red symbols are associated, whereas those denoted with blue symbols are certainly not. The lengths of the cyan lines connecting the unassociated galaxy pairs are substantially larger than their apparent separations in the projected  $X - Y$  plane.

approximate environmental effects near massive clusters, satellite SFRs are reduced by a factor equal to their current subhalo mass divided by the peak mass in their subhalo’s mass accretion history. This is only a toy model for satellite quenching, of course. However, our results should be insensitive to the inclusion of satellite quenching because satellites are typically too submm-faint to contribute to the (detectable) SMG population.

Our method ensures that the mock sample has stellar mass functions, average specific SFRs, cosmic star formation history, and autocorrelation as a function of stellar mass that are consistent with observations. Because the model reproduces the mean SFR for a given stellar mass (including some scatter) and redshift rather than  $\text{SFR}(M_*, z)$  for individual haloes, the elevation in SFR associated with starbursts is not included, so we simply do not treat that subpopulation of SMGs in this work. This issue is discussed in detail in Section 4.5.

## 2.2 Assigning submm flux densities

To assign submm fluxes to the mock galaxies, we use the following fitting function, which was derived using the results of SUNRISE (Jonsson 2006; Jonsson et al. 2010) dust radiative transfer calculations performed on GADGET-3 (Springel 2005) smoothed-particle hydrodynamics simulations of isolated disc and merging galaxies (eq. 15 of H13):

$$S_{850} = 0.81 \text{ mJy} \left( \frac{\text{SFR}}{100 \text{ M}_\odot \text{ yr}^{-1}} \right)^{0.43} \left( \frac{M_d}{10^8 \text{ M}_\odot} \right)^{0.54}, \quad (1)$$

where  $S_{850}$  is the observed-frame 850- $\mu\text{m}$  flux density and  $M_d$  is the dust mass (we describe the method for assigning  $M_d$  below). This function can recover the submm flux of simulated galaxies in

the redshift range  $z \sim 1 - 6$  to within a scatter of 0.13 dex because the negative  $K$ -correction makes the observed-frame  $S_{850}$  of a fixed galaxy SED almost independent of  $z$  in the range  $z \sim 1 - 10$  (e.g., Blain et al. 2002). It under-predicts the flux at lower redshifts, significantly so for  $z \lesssim 0.5$ . However, because the normalization of the  $\text{SFR}-M_*$  relation decreases strongly from  $z \sim 1$  to  $z \sim 0$  (e.g., Noeske et al. 2007; Daddi et al. 2007) and the volume in the range  $z = 0 - 1$  is a small fraction of the total  $z = 0 - 6$  volume, both the observed (e.g., Smolčić et al. 2012a; Yun et al. 2012; Weiß et al. 2013) and predicted (Hayward 2012; H13) fraction of SMGs with  $z \lesssim 1$  is small; thus, this under-prediction should not significantly affect our results. Because the Eddington (1913) bias (see also Hogg & Turner 1998) can affect the shape of the number counts, we incorporate the scatter of 0.13 dex when assigning flux densities to the mock galaxies.

The fitting function requires the SFR and  $M_d$  of each mock galaxy. The SFR is already determined from the Behroozi et al. (2013a) method.<sup>2</sup> To assign dust mass values, we follow the method of H13, in which the gas fraction  $f_g$  and metallicity  $Z$  are parameterized as functions of stellar mass and redshift and it is assumed that 40 per cent of the metals are contained in dust grains. The functional form for  $f_g(M_*, z)$  is physically motivated, and the parameters are constrained to match  $z \lesssim 3$  observations; see Hopkins et al. (2010) for details. The form for  $Z(M_*, z)$  is based

<sup>2</sup> We have checked the effect of calculating the SFR following H13 instead. For the majority of the sources, the SFRs and thus submm flux densities are very similar. Consequently, the results presented here are qualitatively insensitive to this choice, although there can be some quantitative discrepancies at the bright end because of the small number of sources that contribute there.

on the observed stellar mass–metallicity relation at different redshifts; see H13 for details. We note that because  $S_{850}$  scales significantly sublinearly with both SFR and  $M_d$ , the predictions are relatively insensitive to variations in these quantities; e.g., a factor of 2 change in either quantity changes  $S_{850}$  by less than 50 per cent.

### 2.3 Identifying blended sources

Once submm flux densities are assigned to all mock galaxies, we perform a brute-force search for blended multiples. First, we select only those sources with  $S_{850} > 1$  mJy because fainter sources are below the flux density limits of current single-dish surveys and interferometric follow-up observations (e.g., Karim et al. 2013).<sup>3</sup> This flux cut yields a minimum flux density of  $n$  mJy for  $n$ -component blended sources. Then, for each source  $i$  in this subsample, we compute the angular distance to all sources  $j$  in the subsample for which  $j > i$  (to avoid double-counting). If one or more sources is within a ‘beam size’<sup>4</sup> of source  $i$ , which we vary, we consider the sources to be blended and sum their  $S_{850}$  values to calculate the total  $S_{850}$  for the blended source.

For each blended source, we compute a measure of the redshift separation of the components by summing the redshift separations between the first component and all other components in quadrature:

$$\Delta z \equiv \left( \sum_{i>1}^N (z_i - z_1)^2 \right)^{1/2}, \quad (2)$$

where  $z_i$  denotes the redshift of the  $i$ th component and  $N$  is the total number of components of the blended source. This is a somewhat arbitrary (yet natural) measure: for two components,  $\Delta z$  is simply the difference in the redshifts of the two components. For sources with  $> 2$  components,  $\Delta z \gg 0$  indicates that at least one of the components is at significantly different  $z$  than the others. Below, we define ‘spatially associated’ and ‘spatially unassociated’ blended sources by  $\Delta z < 0.02$  and  $\Delta z \geq 0.02$ , respectively. The justification for and insensitivity of our results to the value of this cut are presented in Section 3.3.

Fig. 1 presents a simple illustration of the difference between spatially associated and unassociated projected pairs. The panels show the positions of a sample of mock galaxies projected onto the  $X - Y$  (left) and  $X - Z$  (right) planes. The galaxy pairs marked with red symbols are spatially associated in 3D (and thus also in

projection). In contrast, the galaxy pairs marked with blue symbols appear to be associated in the  $X - Y$  projection, but the  $X - Z$  projection clearly demonstrates that they are spatially unassociated. Without accurate redshifts, an observer viewing these galaxies along the  $Z$  axis cannot distinguish between these two types of projected pairs. This figure also illustrates how the spatial information provided by cosmological simulations is essential for treating the contribution of spatially unassociated projected multiples to the SMG population.

## 3 RESULTS

### 3.1 Cumulative number counts of blended and isolated-disc SMGs

Fig. 2 shows the SMG cumulative number counts ( $\text{deg}^{-2}$ ) versus  $S_{850}$  (mJy) predicted for beam sizes of 15 arcsec (which is representative of the resolution of the single-dish telescopes used to determine the observed counts) and 7 arcsec (for a conservative estimate of the effects of blending) and when blending is not included. The first two curves include blended SMGs and isolated disc SMGs that are not components of blended sources. All counts are the median counts taken over the eight mock catalogues, and the grey dashed error bars correspond to the standard deviation. The black points with solid error bars are observational data (see the caption for details). The simulation data plotted in this figure are presented in Table 1. Observed 1.1-mm counts have been approximately converted to 850- $\mu\text{m}$  counts using  $S_{850} \approx 2.3S_{1.1}$ . This conversion is also used to show approximate  $S_{1.1}$  values on the top axis; see H13 for details.

For the 15-arcsec beam, the predicted counts of blended SMGs are consistent with most of the observed counts for typical SMGs ( $S_{850} \lesssim 6$  mJy) but a factor of  $\sim 5 - 10$  less than the observed counts for  $S_{850} \gtrsim 10$  mJy. The Aretxaga et al. (2011) counts are significantly more discrepant. Aretxaga et al. (2011) argue that the origin of the discrepancy between their counts and others observed for similarly sized fields is the impact of galaxy-galaxy weak lensing due to higher than average matter density along the line of sight. This hypothesis is supported by the association of the excess bright sources with foreground galaxy overdensities at  $z < 1.1$ . We do not include the effects of lensing here and thus would not produce this effect if it is the cause. However, the magnitude of the effect of lensing on the submm counts is still uncertain; see Section 4.5 for further discussion.

The difference between the predictions for the 15-arcsec beam (red solid line) and 7-arcsec beam (blue dashed line) indicates that the total number counts of the blended sources quantitatively depend on the beam size, as one naïvely expects. This suggests that the counts observed by telescopes of different resolutions will differ, as is already known (e.g., Casey et al. 2013). However, the difference also partially reflects uncertainty in the number counts predicted by our model because of our simple treatment of blending (see Section 4.5). Fortunately, there are multiple predictions that are robust to this aspect of the model; we discuss these predictions below.

Note also the significant uncertainty in the  $S_{850} \gtrsim 7 - 10$  mJy counts (depending on the amount of blending), which originates from sample variance and scatter in the SFR–halo mass relation. This affects all the counts, including the ‘no blending’ case, because the maximum overdensity sampled varies with the field. It further affects the counts that include blending by altering the probability that two high-sigma peaks have sufficiently small projected

<sup>3</sup> Sources fainter than the detection limit cause the zero-level of the submm map to be biased. However, this bias can be corrected when deriving number counts from submm maps (see, e.g., section 3.2.3 of Weiß et al. 2009), so we consider it reasonable to ignore the contribution of such sources to the predicted number counts. Using a different flux density limit in our model naturally changes the number of components of individual sources because for a lower (higher) flux density limit, the interferometric follow-up observations would detect more (fewer) components. We have checked the effects of using alternate flux density limits of  $S_{850} = 0.5$  and 2 mJy. The quantitative predictions for the absolute number counts change, but the relative contributions of the subpopulations and the distributions of the redshift separations of components are relatively robust. Furthermore, the conclusions are qualitatively unchanged, and this uncertainty is subdominant to that associated with the treatment of blending.

<sup>4</sup> Throughout this work, we refer to the ‘beam’ and ‘beam size’ used in our model, but it should be understood that we are not claiming to precisely mimic the effects of blending (cf. fig. 1 of Hayward et al. 2012). Rather, our treatment is simply an approximation. This limitation is discussed in Section 4.5.



**Table 1.** Cumulative number counts for different amounts of blending.

$S_{850}^a$ (mJy)	$\sim S_{1.1}^b$ (mJy)	$N_{15''}(> S_{850})^c$ (deg $^{-2}$ )	$N_{7''}(> S_{850})^d$ (deg $^{-2}$ )	$N_{\text{no blend}}(> S_{850})^e$ (deg $^{-2}$ )
2.0	0.9	3084.7 $\pm$ 207.8	1606.6 $\pm$ 69.8	538.3 $\pm$ 21.1
3.0	1.3	1514.3 $\pm$ 174.8	534.2 $\pm$ 48.5	98.0 $\pm$ 6.6
4.0	1.7	715.3 $\pm$ 103.0	180.1 $\pm$ 25.2	24.0 $\pm$ 5.0
5.0	2.2	316.3 $\pm$ 62.5	59.2 $\pm$ 11.1	5.1 $\pm$ 1.4
6.0	2.6	135.2 $\pm$ 30.7	20.9 $\pm$ 5.2	1.5 $\pm$ 0.9
7.0	3.0	56.6 $\pm$ 12.9	7.7 $\pm$ 2.5	0.5 $\pm$ 0.4
8.0	3.5	22.4 $\pm$ 6.6	2.0 $\pm$ 2.0	< 0.5
9.0	3.9	9.2 $\pm$ 2.1	1.0 $\pm$ 0.9	–
10.0	4.3	4.6 $\pm$ 1.6	< 0.5	–
11.0	4.8	2.0 $\pm$ 1.2	–	–
12.0	5.2	1.0 $\pm$ 0.8	–	–
13.0	5.7	< 0.5	–	–

<sup>a</sup> 850- $\mu\text{m}$  flux density. <sup>b</sup> Approximate 1.1-mm flux density calculated using  $S_{1.1} \approx S_{850}/2.3$ . <sup>c</sup> Cumulative 850- $\mu\text{m}$  number counts for a beam size of 15 arcsec. <sup>d</sup> Same as column (3), but for a 7-arcsec beam. <sup>e</sup> Cumulative number counts without the effects of blending included.

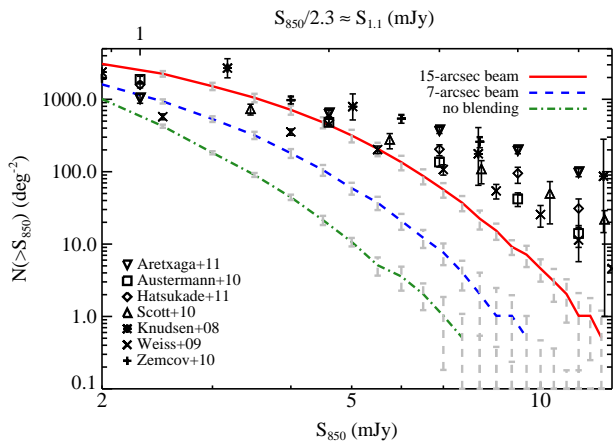


**Figure 2.** Cumulative number counts of model single-dish-detected SMGs (isolated discs and blends of multiple components) versus  $S_{850}$  (mJy) for 15-arcsec (red solid line) and 7-arcsec (blue dashed line) beams. The number counts predicted when blending is not included are shown for comparison (green dot-dashed line). All lines denote the median value taken over the eight mock catalogues, and the grey dashed error bars indicate the standard deviation. The black points with solid error bars indicate the observational data from Aretxaga et al. (2011), Austermann et al. (2010), Hatsukade et al. (2011), Scott et al. (2010), Knudsen, van der Werf, & Kneib (2008), Weiß et al. (2009), and Zemcov et al. (2010); see the legend for the corresponding symbols. The top axis indicates approximate 1.1-mm flux density values calculated using  $S_{1.1} \approx S_{850}/2.3$  (see H13 for details). The predicted counts agree well with those observed for typical SMGs ( $S_{850} \lesssim 6$  mJy), but they are a factor of  $\sim 5 - 10$  less (neglecting those of Aretxaga et al.; see text for details) for  $S_{850} \gtrsim 10$  mJy, which suggests that it is still necessary to include the SFR elevation caused by starbursts to match the observed counts.

separation to be blended. Thus, even for independent fields with areas as large as  $\sim 2$  deg $^2$ , the counts of the brightest sources vary significantly. This effect could be the reason that the Karim et al. (2013) and Smolčić et al. (2012a) samples vary in terms of the maximum flux density of non-blended SMGs. For example, for a  $\sim 1$  deg $^2$  field, the flux density of the brightest non-blended source observed can vary in the range  $S_{850} \sim 6 - 9$  mJy (note that inclusion of starbursts would increase these values), and this effect

is of course more significant for smaller surveys. LESS, the survey from which the sources observed by Karim et al. were drawn, covers an area of 0.25 deg $^2$ , and the Smolčić et al. sources were drawn from the central 0.7 deg $^2$  of the Cosmic Evolution Survey (COSMOS; Scoville et al. 2007) field. Consequently, because the Smolčić et al. survey covered a larger area, the expected flux density for the brightest non-blended SMG in their survey is greater than for the Karim et al. survey.

### 3.2 Relative contributions of spatially associated and unassociated components

Fig. 3 shows the fractional contribution of different subpopulations of blended SMGs to the total blended SMG cumulative number counts (i.e., the cumulative number counts of that subpopulation divided by the total cumulative number counts of blended sources) versus  $S_{850}$ . The values are the medians of the individual ratios for the eight mock catalogues, and the grey dashed error bars indicate the standard deviations. We consider the spatially associated<sup>5</sup> (solid lines) and spatially unassociated (dashed lines) subpopulations, which are defined by  $\Delta z < 0.02$  and  $\Delta z \geq 0.02$ , respectively. (The justification for this value is presented in Section 3.3. Here, we simply note that the results are insensitive to the specific cut because the  $\Delta z$  distribution is strongly bimodal.) For both of the aforementioned subpopulations, the fractional contributions of blended sources composed of two (more than two) components are denoted with blue (red) lines, and the total fractional contributions of associated and unassociated sources (i.e., independent of the number of components) are shown in green.

One of the robust predictions of our model is that both spatially associated and unassociated blended sources contribute significantly at all flux densities and for the range of beam sizes explored. Specifically, we expect that assuming a detection limit of  $S_{870} > 1$  mJy,  $\gtrsim 50$  per cent of blended SMGs contain at least one

<sup>5</sup> ‘Spatially associated’ is a necessary but not sufficient condition for the individual components to be interacting galaxies. However, because a classification based only on the difference(s) in the redshifts of the components will be most easily tested with forthcoming observations, we opt to use this simple criterion rather than a more sophisticated method (e.g., Moreno 2012).

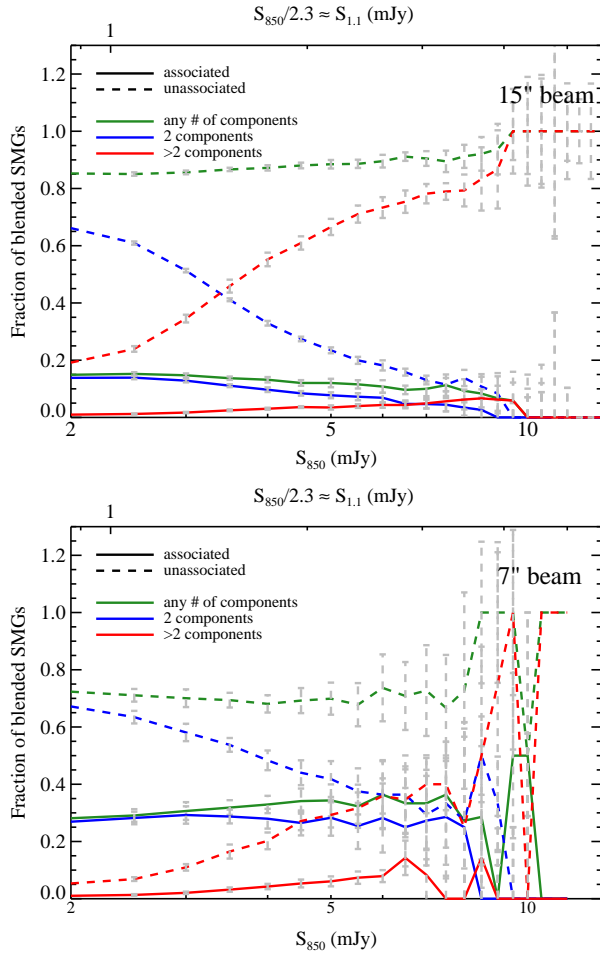


**Figure 3.** Relative contributions of various subpopulations to the cumulative number counts of blended SMGs for 15-arcsec (top) and 7-arcsec (bottom) beams. (Non-blended SMGs are ignored here.) The solid lines indicate blended sources for which all components are spatially associated ( $\Delta z < 0.02$ ), and the dashed lines are for blended SMGs in which at least one component is spatially unassociated ( $\Delta z \geq 0.02$ ). The blue (red) lines correspond to blended SMGs that are composed of 2 (> 2) components, and the (dashed) solid green line denotes the contribution of all (un)associated blended SMGs, regardless of the number of components. The lines indicate the median fraction at a given  $S_{850}$  for the eight mock catalogues, and the grey dashed error bars indicate the standard deviation. At all flux densities plotted, spatially unassociated components contribute to  $\gtrsim 50$  per cent of the blended SMGs. For the 15-arcsec beam, the blended SMGs are dominated by > 2-component sources in which at least one component is spatially unassociated. The contribution of spatially unassociated components increases with the beam size.

component that is spatially unassociated with the others. The fractional contribution varies with the flux density and beam size and may be sensitive to the treatment of blending, but the significance of the contribution is robust. For the 15-arcsec beam, the blended SMGs with  $S_{850} \gtrsim 3$  mJy are dominated by > 2-component sources for which at least one component is spatially unassociated with the others. In contrast, for the 7-arcsec beam, the typical blended SMG in our model is composed of two unassociated galaxies.

Fig. 3 also indicates that the relative contribution of spatially unassociated sources is greater for the 15-arcsec beam, especially for the > 2-component sources. This is simply because the greater

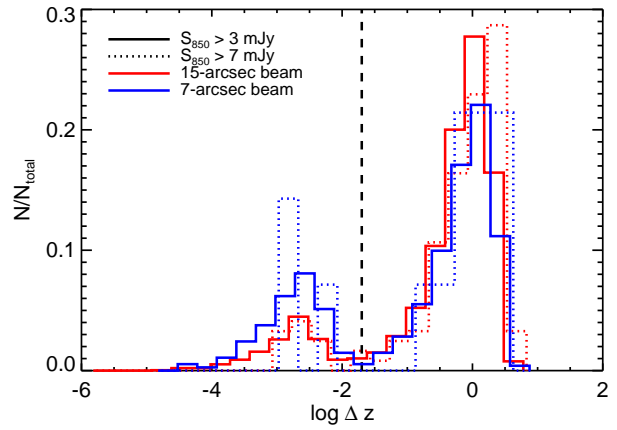


**Figure 4.** The solid (dotted) lines show the distribution of the logarithm of the redshift separation of the individual components (as defined in Eq. 2) of the blended submm sources in one of the mock lightcones with total blended flux density  $S_{850} > 3$  (7) mJy for both the 15-arcsec (red) and 7-arcsec (blue) beams. The distribution is strongly bimodal, which justifies the  $\Delta z$  cut used to separate the spatially associated and unassociated subpopulations; this cut ( $\Delta z = 0.02$ ) is indicated by the vertical dashed line. The median values are  $\Delta z \sim 0.9 - 1.5$ , depending on the beam size and flux cut (see Table 2). Note that the shapes of the distributions are relatively insensitive to the beam size, although for the 7-arcsec beam, a higher fraction of the sources are spatially associated.

**Table 2.** Median  $\Delta z$  values.

Beam size (arcsec)	$S_{850} > 3$ mJy <sup>a</sup>	$S_{850} > 7$ mJy <sup>b</sup>
15	$0.99 \pm 0.02$	$1.46 \pm 0.16$
7	$0.87 \pm 0.06$	$1.00 \pm 0.35$

<sup>a</sup> Median and standard deviation of the  $\Delta z$  values for each of the eight mock catalogues of blended SMGs with  $S_{850} > 3$  mJy and for the beam size specified in column (1). <sup>b</sup> Same as column (2), but for  $S_{850} > 7$  mJy.

beam size increases the likelihood of multiple physically and spatially unassociated galaxies falling within the same beam. In contrast, the relative contribution of spatially associated blended SMGs is less for the 15-arcsec beam for two reasons: 1. The number of additional physically associated galaxies blended when the beam size is 15 arcsec is relatively small because the projected separation of such systems is typically less than the 7-arcsec beam (i.e.,  $\sim 65$  kpc at  $z \sim 2 - 3$ ); thus, the 7-arcsec beam is sufficient to blend these sources. 2. Some sources that are spatially associated for the 7-arcsec beam become classified as spatially unassociated for the 15-arcsec beam because one or more additional, spatially unassociated galaxies become blended with the spatially associated sources when the beam size is increased to 15 arcsec. For the same reason, the number of sources with > 2 components is significantly greater when the beam size is 15 arcsec.

### 3.3 Redshift separations of the components of blended SMGs

The final testable prediction that we make concerns the distribution of the redshift separation of the individual components of blended SMGs. Fig. 4 shows the distributions of  $\log \Delta z$  for blended sources that are brighter than two different flux cuts,  $S_{850} > 3$  (solid lines)

and 7 (dotted lines) mJy for both beam sizes (15 arcsec in red and 7 arcsec in blue). The distributions are strongly bimodal (we interpret this bimodality below), and there is a clear minimum at  $\Delta z \sim 0.02$  (marked by the vertical dashed line), which is why we use this value as the cut to distinguish the spatially associated and unassociated subpopulations. (Using a smaller, more physically meaningful cut, such as  $\Delta z = 0.01$ , does not significantly alter the results because of the strong bimodality.) As discussed above, for the 7-arcsec beam, a higher fraction of the sources are spatially associated.

Many of the galaxies in the spatially associated subpopulation ( $\Delta z < 0.02$ ) are also physically associated, i.e., gravitationally bound galaxies that will merge. The galaxy-pair SMGs (early-stage mergers) discussed in detail in Hayward et al. (2012) and H13 are a subset of the spatially associated galaxies. This category also involves galaxies that are undergoing fly-by encounters but will not merge. Typically, the spatially associated galaxies are in distinct haloes, and the separations can be as large as  $\sim 10$  Mpc (comoving). The spatially unassociated galaxies ( $\Delta z \geq 0.02$ ) include at least one component that is simply a chance projection, i.e., is completely unrelated with the other(s). The separations amongst the components of the spatially unassociated galaxies range from a few Mpc to the box size.

The median and standard deviation of the  $\Delta z$  values (calculated from the individual values for each mock catalogue) for the spatially unassociated subpopulations are listed in Table 2. Note that the median values are of order 1, which is a natural consequence of the redshift distribution of SMGs in our model: most SMGs are in the range  $z \sim 2 - 4$ , and the median redshift is  $\sim 3$ .<sup>6</sup> Thus, the typical separation of components is naturally  $\sim 1$ . The median value of  $\Delta z$  is relatively insensitive to the beam size, flux density cut, and mock catalogue used; thus, it is a robust, testable prediction of our model. The maximum  $\Delta z$  varies significantly for the different mock catalogues and ranges from  $z \sim 4 - 6$ .

## 4 DISCUSSION

### 4.1 Can the brightest SMGs be explained via blending alone?

The recent observational evidence (Karim et al. 2013; Smolčić et al. 2012a) that many of the single-dish SMGs with  $S_{870} \gtrsim 12$  mJy are blends of multiple components was part of the impetus for this work. In particular, we sought to address whether our model could predict a sufficient number of blended SMGs to account for the observed number counts of sources with  $S_{870} \gtrsim 12$  mJy because in the H13 model, such sources are predominantly starbursts (the models are compared in detail in Section 4.4).

By including the contribution from spatially unassociated components (i.e., chance projections), we predict blended SMG number counts (for a 15-arcsec beam) that are consistent with the observed counts within the uncertainties for typical ( $S_{850} \lesssim 6$  mJy)

<sup>6</sup> At  $z \lesssim 2$ , the SFRs and (thus submm fluxes) of star-forming galaxies are significantly lower (e.g., Noeske et al. 2007; Daddi et al. 2007; Magnelli et al. 2009, 2011; Karim et al. 2011; Whitaker et al. 2012), a significant fraction of massive galaxies have been quenched (e.g., Bell et al. 2004, 2007; Faber et al. 2007; Ilbert et al. 2010, 2013; Davidzon et al. 2013), and the volume probed is relatively small; all of these reasons cause the SMG counts to drop significantly at  $z \lesssim 2$ . At  $z \gtrsim 4$ , the scarcity of massive galaxies and decreased dust content of galaxies causes the counts to decrease. See Hayward 2012 and H13 for more details.

SMGs but a factor of  $\sim 5 - 10$  less than the observed counts for the brightest ( $S_{850} \gtrsim 10$  mJy) sources (ignoring the Aretxaga et al. 2011 counts, which are thought to be significantly boosted by weak lensing, as discussed above). The underprediction at the bright end suggests that inclusion of the SFR elevation caused by starbursts is still necessary to reproduce the brightest sources, regardless of whether those sources are blends of multiple components. Furthermore, we must account for the sources with  $S_{870} \gtrsim 12$  mJy that are clearly not blended sources, because some examples are known (see Hayward 2013 for further discussion); it is very difficult to explain such objects without invoking starbursts induced by major mergers or disc instabilities. Both issues are deferred to future work, which we outline below.

### 4.2 The importance of mock observations for testing models

We have seen that a given single-dish-detected SMG can actually correspond to multiple physical galaxies.<sup>7</sup> However, it is often assumed that an SMG corresponds to a single (real or model) galaxy. Although this assumption is valid for isolated discs and reasonable for late-stage mergers, it is questionable for early-stage mergers, in which the progenitor discs are well separated and not yet strongly interacting, and definitely invalid for projected multiples. This error, which is commonly committed by theoreticians but better understood amongst observers, can be partially attributed to the term ‘submillimetre galaxy’, which is somewhat misleading.<sup>8</sup>

Were this simply a matter of terminology, it would not be a concern, because the astronomical literature is rife with misleading terminology. However, equating SMGs with individual ‘galaxies’ in simulations or semi-analytical models (SAMs) can lead to *qualitatively* inaccurate conclusions because of the significant differences between predictions for individual model galaxies (e.g., the ‘no blending’ curve in Fig. 2) and predictions for model SMGs (e.g., the other curves in Fig. 2); to make predictions that are classified into the latter category, a model must attempt to at least crudely mimic observations. This model-comparison problem is not specific to SMGs, of course (see, e.g., Lotz et al. 2008, 2010a,b; Wuyts et al. 2009, 2010; Scannapieco et al. 2010; Snyder et al. 2011, 2013), but it is especially acute for them because 1. observations of SMGs are more limited than for local and/or less dusty galaxies and 2. the small dynamic range of submm flux density currently probed and the steepness of the number counts implies that relatively small changes in flux density – caused by, e.g., blending – can qualitatively affect the conclusions. Because of the large beam sizes that are characteristic of far-IR observations, other far-IR-selected populations (e.g., ‘hot-dust ULIRGs’; Chapman et al. 2004; Casey et al. 2009, 2011) should also be affected by the blending effects discussed here.

### 4.3 Implications for the inferred SFRs of SMGs

Properly treating blending may reconcile the longstanding discrepancy between the far-IR and (sub)mm counts predicted by cosmological simulations and SAMs and those observed. Furthermore,

<sup>7</sup> By ‘galaxy’, we refer to a virialized dark matter halo that contains baryons; see Willman & Strader (2012) for a more observationally motivated definition.

<sup>8</sup> Perhaps ‘submillimetre source’ is a better term, but the acronym ‘SMS’ is already widely used for another purpose.

the possible ubiquity of blended submm sources has an important implication for interpreting SMG observations: if many of the brightest sources are actually multiple unrelated galaxies, the SFRs inferred under the assumption that a single submm source corresponds to a single galaxy would overestimate the true SFRs of individual galaxies. Such an overestimate of the abundance of the most rapidly star-forming galaxies may relieve the tension between the SFRs of the mock SMGs in the cosmological simulation of Davé et al. (2010) and those inferred from single-dish observations.

To obtain the true SFRs of individual galaxies, resolved photometry of the individual components is required. In the UV-optical, this process is limited by the significant attenuation that is characteristic of SMGs. In the IR-(sub)mm, the resolution is the limitation. The ALMA continuum measurements from the LESS follow-up survey (Karim et al. 2013; Hodge et al. 2013) will help in this regard, but additional high-resolution data in the far-IR, particularly shortward of the peak of the dust emission, are necessary to accurately constrain the IR luminosity and thus infer the SFRs of the individual components. Therefore, the question of whether the SFRs of galaxies in cosmological simulations and real galaxies are in tension should be revisited when possible.

#### 4.4 Comparison with the H13 model

Although the model presented in this work and that of H13 have some ingredients in common, they differ in the following important aspects: (1) Here, we directly include information about large-scale structure by using mock galaxy catalogues generated from the *Bolshoi* simulation. In H13, the cosmological context was obtained solely through the use of merger rates calibrated to cosmological simulations and an assumed stellar mass function. Consequently, no spatial information was included, and thus chance projections of spatially unassociated galaxies could not be treated. (2) In H13, the effects of blending were included for early-stage mergers, but in a cruder manner (by assuming a fixed timescale) than in this work. (3) Because the procedure to generate the mock galaxy catalogues relies on an SFR-halo mass relation (that depends on redshift and includes some scatter), the full SFR enhancement caused by merger-induced starbursts is not included in this work. In H13, the submm light curves for merger-induced starbursts were directly calculated by performing dust radiative transfer on hydrodynamical simulations. Consequently, the SFR enhancement in such objects was treated in the H13 model.

The differences described above imply that neither the H13 model nor that presented here can fully treat all proposed SMG subpopulations. Thus, the predictions of the two models cannot be directly compared. However, additional insight can be obtained by combining some of their results. Here, we have demonstrated that blending of unassociated galaxies can significantly boost the submm number counts. Thus, our results reinforce the conclusion of H13 that given a demographically accurate model galaxy population (i.e., one with stellar mass functions and merger rates consistent with observations), the observed submm counts can be matched without recourse to variation in the stellar initial mass function. Furthermore, if spatially unassociated multiples were included in the H13 model, it is possible that the model would overpredict the observed counts. Such an overprediction could imply that the normalisation of the stellar mass function used in the H13 model is too high or that the H13 simulations are missing some important form of feedback that limits the SFR in starbursts.

#### 4.5 Limitations of our model

The strength of the model presented in this work is that it naturally includes information about large-scale structure and thus enables us to physically characterise the effects of blending for both spatially associated and unassociated galaxies; in contrast, H13 treated only the blending of the components of early-stage mergers, and the treatment was significantly cruder. However, the method used here naturally also has some limitations.

First, the method by which we assign SFRs to galaxies treats scatter in the SFR-halo mass relation at a given mass and redshift, but it does not faithfully reproduce the SFR evolution of individual haloes. In particular, the elevation in SFR associated with merger-induced starbursts (i.e., the high-SFR tail at a given halo mass), which is generically predicted by idealised simulations of major mergers (e.g., Hernquist 1989; Barnes & Hernquist 1991, 1996; Mihos & Hernquist 1996; Springel, Di Matteo, & Hernquist 2005; Cox et al. 2006; Younger et al. 2009b), is not included. It would be possible to include this effect in an empirically motivated manner (e.g., Béthermin et al. 2012). However, because merger-induced starbursts were treated extensively in H13, and the primary focus of this work is to investigate the contribution of spatially unassociated components to blended SMGs, we opt to simply neglect merger-induced starbursts here.

Subsets of the spatially associated 2-component and both spatially associated and unassociated  $> 2$ -component blended SMGs should be undergoing merger-induced starbursts. (The reason that some of the spatially unassociated  $> 2$ -component blended SMGs should be undergoing starbursts is that in those sources, a subset of the components can be spatially and physically related.) Because we do not include the elevation in SFR from starbursts, we underestimate the submm fluxes of such objects. However, because the duty cycle of the starburst phase is significantly less than that of the ‘galaxy-pair SMG’ phase (H13), the galaxies are not likely to be resolved into separate components during the strong starburst phase, and not all encounters cause starbursts, the fraction of blended SMGs that are undergoing starbursts should be relatively small. For more typical spatially associated multiples, which have large separations (i.e.,  $\gtrsim 10$  kpc), the SFR elevation should be relatively modest (e.g., Scudder et al. 2012; Lanz et al. 2013; Patton et al. 2013). Consequently, our conclusions regarding the relative contributions of spatially associated and unassociated components to blended SMGs and the distributions of the redshift separations of the components would not be significantly affected by the inclusion of starbursts (but the quantitative predictions regarding, e.g., the number counts should be affected, and the conclusions regarding the brightest sources may differ). Still, there is strong observational evidence that galaxies above the main sequence (i.e., merger-induced starbursts and gravitationally unstable disc galaxies) contribute to the SMG population (e.g., Magnelli et al. 2012; Michałowski et al. 2012), and H13 predicted a significant starburst contribution to the SMG population. Thus, we should and will address this shortcoming of the model presented here in future work.

Furthermore, the treatment of blending is still somewhat crude, albeit significantly less crude than that used in H13 and far superior to simply ignoring blending. The difference between the predicted counts for the 15- and 7-arcsec beam sizes illustrated by Fig. 2 indicates that the treatment of blending can significantly affect some predictions of the model. Although there should certainly be differences in the blended SMG populations identified using telescopes of different beam sizes, the predictions for a given beam size in the model should not be considered to exactly correspond to



observations from a telescope of the same beam size. Rather, for the typical single-dish SMG surveys, which have been performed with telescopes with  $\sim 15$ -arcsec beams, our predictions for the 15- and 7-arcsec beams should be considered somewhat liberal and very conservative estimates of the number counts of blended SMGs, respectively.

Finally, we have neglected the effects of gravitational lensing on the predicted number counts. As already mentioned above, Aretxaga et al. (2011) suggest that galaxy-galaxy lensing is the reason that their counts are significantly higher than those for other fields (see also Austermann et al. 2009). Furthermore, a population of strongly lensed SMGs has been observed (Vieira et al. 2010). However, the effect of lensing for sources with  $S_{850} \lesssim 10$  mJy is poorly constrained: estimates of the typical magnification for such sources range from  $\sim 10$  per cent (e.g., Paciga, Scott, & Chapin 2009; Lima et al. 2010b; Lima, Jain, & Devlin 2010a) to of order 10 (Harris et al. 2012). Thus, we have opted to defer a treatment of lensing to future work.

#### 4.6 Future work

In future work, we will combine our fitting function for submm flux density with an updated version of the SAM of Somerville et al. (2008) and Somerville et al. (2012) to produce mock submm maps of the galaxies from the SAM. Then, to make predictions for various telescopes, we will convolve the maps with the appropriate beams. This approach will enable us to simultaneously treat the isolated disc, merger-induced starburst, and both spatially associated and unassociated blended SMG subpopulations in order to present a more complete picture of the SMG population. Furthermore, we will investigate the effects of modifying the prescriptions in the SAM for, e.g., star formation and feedback on the mock SMG population. The spatial information available in our mock SMG catalogues makes them a natural tool for investigating SMG clustering and the effects of lensing on submm number counts. Finally, we will complement our semi-analytic approach through the use of state-of-the-art cosmological hydrodynamical simulations (Vogelsberger et al. 2013; Torrey et al. 2013).

## 5 CONCLUSIONS

We created mock SMG catalogues by generating lightcones from the *Bolshoi* simulation, assigning SFRs and dust masses to the mock galaxies in an empirically constrained manner, and using a fitting function from previous work to assign submm flux densities. Then, the mock SMG catalogues were used to investigate the effects of blending of multiple galaxies on the SMG population. Our principal conclusions are the following:

(i) For the 15-arcsec beam, the predicted counts of blended SMGs are consistent with most of the observed counts for typical SMGs ( $S_{850} \lesssim 6$  mJy) but a factor of  $\sim 5 - 10$  less than the observed counts for  $S_{850} \gtrsim 10$  mJy. The underprediction at the bright end suggests that inclusion of the SFR elevation caused by starbursts is still necessary to reproduce the brightest sources, regardless of whether those sources are blends of multiple components.

(ii) The difference in the maximum flux density of non-blended SMGs in the Smolčić et al. (2012a), Karim et al. (2013), and Barger et al. (2012) samples is consistent with the variation in the flux density of the brightest non-blended SMG amongst our mock

SMG catalogues. Thus, the difference may simply be a consequence of sample variance and scatter in the SFR–halo mass relation.

(iii) Both spatially associated and unassociated blended SMGs contribute significantly to the population:  $\gtrsim 50$  percent of the blended SMGs in our model contain one or more components with  $S_{850} > 1$  mJy that are spatially distinct from the other(s). The fractional contribution depends on both the flux density and beam size. For a 15-arcsec beam, blends of  $> 2$  galaxies in which at least one galaxy is spatially unassociated with the others dominate the blended sources with total  $S_{850} > 3$  mJy.

(iv) The distribution of the redshift separations of the components of blended SMGs is strongly bimodal. For the spatially unassociated subpopulation, the median redshift separation is in the range  $\Delta z \sim 0.9 - 1.5$ , depending on the beam size and flux cut.

We stress that the last two conclusions are bona fide predictions in the sense that (to our knowledge) currently available observational data are insufficient to test them, but they will be tested as soon as spectroscopic or sufficiently accurate photometric redshifts of the individual components of a sufficient number of blended SMGs are available.

## ACKNOWLEDGMENTS

We thank Michał Michałowski, Ian Smail, and Volker Springel for comments on the manuscript, Jackie Hodge for useful discussion, and the anonymous reviewer for comments that helped improve the manuscript. CCH is grateful to the organisers of The 30th Jerusalem Winter School in Theoretical Physics, which stimulated discussions that led to this work, to the Klaus Tschira Foundation for financial support, and for the hospitality of the Aspen Center for Physics, which is supported by the National Science Foundation Grant No. PHY-1066293. PSB and RHW received support from HST Theory Grant HST-AR-12159.01-A, provided by NASA through a grant from the Space Telescope Science Institute, which is operated by the Association of Universities for Research in Astronomy, Incorporated, under NASA contract NAS5-26555. JRP acknowledges support from a U.S. National Science Foundation Astronomy and Astrophysics Research Grant (NSF-AST-1010033). JM acknowledges funding from the Canadian Institute for Theoretical Astrophysics and the Natural Sciences and Engineering Research Council of Canada (Discovery Grant; PI: S. L. Ellison).

## REFERENCES

- Aretxaga I. et al., 2011, MNRAS, 415, 3831
- Austermann J. E. et al., 2009, MNRAS, 393, 1573
- Austermann J. E. et al., 2010, MNRAS, 401, 160
- Barger A. J., Wang W.-H., Cowie L. L., Owen F. N., Chen C.-C., Williams J. P., 2012, ApJ, 761, 89
- Barnes J., Hernquist L., 1991, ApJL, 370, L65
- Barnes J., Hernquist L., 1996, ApJ, 471, 115
- Baugh C. M., Lacey C. G., Frenk C. S., Granato G. L., Silva L., Bressan A., Benson A. J., Cole S., 2005, MNRAS, 356, 1191
- Behroozi P. S., Wechsler R. H., Conroy C., 2013a, ApJ, 770, 57
- Behroozi P. S., Wechsler R. H., Wu H.-Y., 2013b, ApJ, 762, 109
- Behroozi P. S., Wechsler R. H., Wu H.-Y., Busha M. T., Klypin A. A., Primack J. R., 2013c, ApJ, 763, 18
- Bell E. F. et al., 2004, ApJ, 608, 752
- Bell E. F., Zheng X. Z., Papovich C., Borch A., Wolf C., Meisenheimer K., 2007, ApJ, 663, 834
- Béthermin M. et al., 2012, ApJL, 757, L23

- Blain A. W., Smail I., Ivison R. J., Kneib J.-P., Frayer D. T., 2002, *Phys-Rep*, 369, 111
- Bothwell M. S. et al., 2010, *MNRAS*, 405, 219
- Casey C. M. et al., 2009, *MNRAS*, 399, 121
- Casey C. M., Chapman S. C., Smail I., Alaghband-Zadeh S., Bothwell M. S., Swinbank A. M., 2011, *MNRAS*, 411, 2739
- Casey C. M. et al., 2013, arXiv:1302.2619
- Chakrabarti S., Fenner Y., Cox T. J., Hernquist L., Whitney B. A., 2008, *ApJ*, 688, 972
- Chapman S. C. et al., 2010, *MNRAS*, 409, L13
- Chapman S. C., Smail I., Blain A. W., Ivison R. J., 2004, *ApJ*, 614, 671
- Cox T. J., Jonsson P., Primack J. R., Somerville R. S., 2006, *MNRAS*, 373, 1013
- Daddi E. et al., 2007, *ApJ*, 670, 156
- Dannerbauer H., Lehnert M. D., Lutz D., Tacconi L., Bertoldi F., Carilli C., Genzel R., Menten K., 2002, *ApJ*, 573, 473
- Davé R., Finlator K., Oppenheimer B. D., Fardal M., Katz N., Kereš D., Weinberg D. H., 2010, *MNRAS*, 404, 1355
- Davidzon I. et al., 2013, arXiv:1303.3808
- Eddington A. S., 1913, *MNRAS*, 73, 359
- Engel H. et al., 2010, *ApJ*, 724, 233
- Faber S. M. et al., 2007, *ApJ*, 665, 265
- Fontanot F., Monaco P., Silva L., Grazian A., 2007, *MNRAS*, 382, 903
- Granato G. L., Lacey C. G., Silva L., Bressan A., Baugh C. M., Cole S., Frenk C. S., 2000, *ApJ*, 542, 710
- Harris A. I. et al., 2012, *ApJ*, 752, 152
- Hatsukade B. et al., 2011, *MNRAS*, 411, 102
- Hayward C. C., 2012, PhD thesis, Harvard University
- Hayward C. C., 2013, *MNRAS*, 432, L85
- Hayward C. C., Jonsson P., Kereš D., Magnelli B., Hernquist L., Cox T. J., 2012, *MNRAS*, 424, 951
- Hayward C. C., Kereš D., Jonsson P., Narayanan D., Cox T. J., Hernquist L., 2011a, *ApJ*, 743, 159
- Hayward C. C., Narayanan D., Jonsson P., Cox T. J., Kereš D., Hopkins P. F., Hernquist L., 2011b, in ASP Conf. Ser. 440, *Have Observations Revealed a Variable Upper End of the Initial Mass Function?*, M. Treyer, T. Wyder, J. Neill, M. Seibert, & J. Lee, ed., ASP, San Francisco, CA, p. 369
- Hayward C. C., Narayanan D., Kereš D., Jonsson P., Hopkins P. F., Cox T. J., Hernquist L., 2013, *MNRAS*, 428, 2529
- Hernquist L., 1989, *Nat*, 340, 687
- Hodge J. A., Carilli C. L., Walter F., de Blok W. J. G., Riechers D., Daddi E., Lentati L., 2012, *ApJ*, 760, 11
- Hodge J. A. et al., 2013, *ApJ*, 768, 91
- Hogg D. W., Turner E. L., 1998, *PASP*, 110, 727
- Hopkins P. F., Younger J. D., Hayward C. C., Narayanan D., Hernquist L., 2010, *MNRAS*, 402, 1693
- Ilbert O. et al., 2013, arXiv:1301.3157
- Ilbert O. et al., 2010, *ApJ*, 709, 644
- Jonsson P., 2006, *MNRAS*, 372, 2
- Jonsson P., Groves B. A., Cox T. J., 2010, *MNRAS*, 403, 17
- Karim A. et al., 2011, *ApJ*, 730, 61
- Karim A. et al., 2013, *MNRAS*, 432, 2
- Klypin A. A., Trujillo-Gomez S., Primack J., 2011, *ApJ*, 740, 102
- Knudsen K. K., van der Werf P. P., Kneib J.-P., 2008, *MNRAS*, 384, 1611
- Komatsu E. et al., 2011, *ApJS*, 192, 18
- Kravtsov A. V., Klypin A. A., Khokhlov A. M., 1997, *ApJS*, 111, 73
- Lanz L. et al., 2013, *ApJ*, 768, 90
- Lima M., Jain B., Devlin M., 2010a, *MNRAS*, 406, 2352
- Lima M., Jain B., Devlin M., Aguirre J., 2010b, *ApJL*, 717, L31
- Lotz J. M., Jonsson P., Cox T. J., Primack J. R., 2008, *MNRAS*, 391, 1137
- Lotz J. M., Jonsson P., Cox T. J., Primack J. R., 2010a, *MNRAS*, 404, 590
- Lotz J. M., Jonsson P., Cox T. J., Primack J. R., 2010b, *MNRAS*, 404, 575
- Magnelli B., Elbaz D., Chary R. R., Dickinson M., Le Borgne D., Frayer D. T., Willmer C. N. A., 2009, *A&A*, 496, 57
- Magnelli B., Elbaz D., Chary R. R., Dickinson M., Le Borgne D., Frayer D. T., Willmer C. N. A., 2011, *A&A*, 528, A35
- Magnelli B. et al., 2010, *A&A*, 518, L28
- Magnelli B. et al., 2012, *A&A*, 539, A155
- Michałowski M. J., Dunlop J. S., Cirasuolo M., Hjorth J., Hayward C. C., Watson D., 2012, *A&A*, 541, A85
- Michałowski M. J., Hjorth J., Watson D., 2010a, *A&A*, 514, A67
- Michałowski M. J., Watson D., Hjorth J., 2010b, *ApJ*, 712, 942
- Mihos J. C., Hernquist L., 1996, *ApJ*, 464, 641
- Moreno J., 2012, *MNRAS*, 419, 411
- Narayanan D., Bothwell M., Davé R., 2012, *MNRAS*, 426, 1178
- Narayanan D., Cox T. J., Hayward C. C., Younger J. D., Hernquist L., 2009, *MNRAS*, 400, 1919
- Narayanan D., Davé R., 2012, *MNRAS*, 423, 3601
- Narayanan D. et al., 2010a, *MNRAS*, 407, 1701
- Narayanan D., Hayward C. C., Cox T. J., Hernquist L., Jonsson P., Younger J. D., Groves B., 2010b, *MNRAS*, 401, 1613
- Niemi S.-M., Somerville R. S., Ferguson H. C., Huang K.-H., Lotz J., Koekemoer A. M., 2012, *MNRAS*, 421, 1539
- Noeske K. G. et al., 2007, *ApJL*, 660, L43
- Paciga G., Scott D., Chapin E. L., 2009, *MNRAS*, 395, 1153
- Patton D. R., Torrey P., Ellison S. L., Mendel J. T., Scudder J. M., 2013, *MNRAS*, in press, arXiv:1305.1595
- Planck Collaboration et al., 2013a, arXiv:1303.5062
- Planck Collaboration et al., 2013b, arXiv:1303.5076
- Primack J. R., 2012, *Annalen der Physik*, 524, 535
- Riechers D. A. et al., 2011a, *ApJL*, 733, L11
- Riechers D. A., Hodge J., Walter F., Carilli C. L., Bertoldi F., 2011b, *ApJL*, 739, L31
- Scannapieco C., Gadotti D. A., Jonsson P., White S. D. M., 2010, *MNRAS*, 407, L41
- Scott K. S. et al., 2010, *MNRAS*, 405, 2260
- Scoville N. et al., 2007, *ApJS*, 172, 1
- Scudder J. M., Ellison S. L., Torrey P., Patton D. R., Mendel J. T., 2012, *MNRAS*, 426, 549
- Shimizu I., Yoshida N., Okamoto T., 2012, *MNRAS*, 427, 2866
- Siringo G. et al., 2009, *A&A*, 497, 945
- Smolčić V. et al., 2012a, *A&A*, 548, A4
- Smolčić V. et al., 2012b, *ApJS*, 200, 10
- Snyder G. F., Cox T. J., Hayward C. C., Hernquist L., Jonsson P., 2011, *ApJ*, 741, 77
- Snyder G. F., Hayward C. C., Sajina A., Jonsson P., Cox T. J., Hernquist L., Hopkins P. F., Yan L., 2013, *ApJ*, 768, 168
- Somerville R. S., Gilmore R. C., Primack J. R., Domínguez A., 2012, *MNRAS*, 423, 1992
- Somerville R. S., Hopkins P. F., Cox T. J., Robertson B. E., Hernquist L., 2008, *MNRAS*, 391, 481
- Springel V., 2005, *MNRAS*, 364, 1105
- Springel V., Di Matteo T., Hernquist L., 2005, *MNRAS*, 361, 776
- Tacconi L. J. et al., 2008, *ApJ*, 680, 246
- Tacconi L. J. et al., 2006, *ApJ*, 640, 228
- Torrey P., Vogelsberger M., Genel S., Sijacki D., Springel V., Hernquist L., 2013, arXiv:1305.4931
- Vieira J. D. et al., 2010, *ApJ*, 719, 763
- Vogelsberger M., Genel S., Sijacki D., Torrey P., Springel V., Hernquist L., 2013, arXiv:1305.2913
- Wagg J. et al., 2012, *ApJL*, 752, L30
- Wang W.-H., Cowie L. L., Barger A. J., Williams J. P., 2011, *ApJL*, 726, L18
- Weiß A. et al., 2013, *ApJ*, 767, 88
- Weiß A. et al., 2009, *ApJ*, 707, 1201
- Whitaker K. E., van Dokkum P. G., Brammer G., Franx M., 2012, *ApJL*, 754, L29
- Willman B., Strader J., 2012, *AJ*, 144, 76
- Wuyts S., Cox T. J., Hayward C. C., Franx M., Hernquist L., Hopkins P. F., Jonsson P., van Dokkum P. G., 2010, *ApJ*, 722, 1666
- Wuyts S. et al., 2009, *ApJ*, 700, 799
- Younger J. D. et al., 2008a, *MNRAS*, 387, 707
- Younger J. D. et al., 2007, *ApJ*, 671, 1531
- Younger J. D. et al., 2009a, *ApJ*, 704, 803
- Younger J. D. et al., 2008b, *ApJ*, 688, 59

Younger J. D., Hayward C. C., Narayanan D., Cox T. J., Hernquist L.,  
Jonsson P., 2009b, MNRAS, 396, L66  
Yun M. S. et al., 2012, MNRAS, 420, 957  
Zemcov M., Blain A., Halpern M., Levenson L., 2010, ApJ, 721, 424